Baryon production and decay into strange-particle final states in 200-GeV/c $\pi^- N$ interactions

H. C. Fenker and D. R. Green
Fermi National Accelerator Laboratory, Batavia, Illinois 60510*

T. Y. Chen,† W. Dieterlie, E. W. Jenkins, K. W. Lai, J. LeBritton,‡ Y. C. Lin,§ and A. E. Pifer
University of Arizona, Tucson, Arizona 85721

J. R. Albright, J. H. Goldman, S. L. Hagopian, J. E. Lannutti, and J. E. Piper
Florida State University, Tallahassee, Florida 32306

C. C. Chang, T. C. Davis, R. N. Diamond,** K. J. Johnson,†† and J. A. Poirier
University of Notre Dame, Notre Dame, Indiana 46556

A. Napier and J. Schneps
Tufts University, Medford, Massachusetts 02155

J. M. Marraffino, J. W. Waters, M. S. Webster, and E. G. H. Williams
Vanderbilt University, Nashville, Tennessee 37235

J. R. Ficenec and W. P. Trower
Virginia Polytechnic Institute and State University, Blacksburg, Virginia 24061
(Received 9 January 1984)

Baryon production and subsequent decay into $K_s^0\Lambda^0$, $\Lambda^0\pi^\pm$, $K_s^0\Lambda^0\pi^\pm$, and $\Lambda^0\pi^+\pi^-$ final states is studied. Evidence for the states $N(1710)$, $\Sigma(1385)$, $\Sigma(1620)$, $\Sigma(1690)$, $\Sigma(2250)$, $\Xi(1320)$, $\Xi(1530)$, $\Xi(1820)$, and $\Xi(1940)$ is presented. Ratios of x_f distributions and cross sections are compared to the predictions of phenomenological models.

It has been observed that resonance production is a source of a substantial fraction of all final-state stable hadrons.[1] Presumably the production characteristics of these resonances form a more direct probe of the underlying production dynamics than do those of the final-state particles. In particular, the ratios of cross sections for resonances with different strangeness should probe local compensation of quantum number.[2] The ratios of x_f distributions provide tests of dimensional-counting rules.[3]

The experiment and data-analysis procedure have been described elsewhere.[4] The data consist of $\sim$60 000 events of the type $\pi^- N \to V^0 V^0 X$ where, $V^0 = K_S^0$, Λ^0, or $\overline{\Lambda}{}^0$, and the charged multiplicity of the X state is required to be less than six. The apparatus is most sensitive to V^0's and charged tracks with $x_f \geq 0.2$; however, produced particles with $x_f \geq 0.0$ are detected and are included in this analysis. The mass resolution of the K_S is ± 5 MeV/c^2 for a typical momentum, $\langle P_{K_S} \rangle \sim 40$ GeV/c. Constrained fits were made to the decay vertex [one constraint (1C)], V^0 mass (1C), and V^0-V^0 primary vertex (1C). Fits were accepted if the χ^2 probability was $\geq 10^{-5}$. The V^0 identification was done by attempting K_S, Λ^0, and $\overline{\Lambda}{}^0$ hypotheses and assigning the best-fit hypothesis. A 5% contamination of $K_S K_S$ is estimated to exist in the $K_S\Lambda^0$, $K_S\overline{\Lambda}{}^0$ sample ($\sim$18 000 events) reported here.

Tracks within the spectrometer are placed into two categories. Tracks passing within $\pm 3\sigma$ of the production target are defined to be "direct" tracks. Those outside this cut are defined to be "decay" tracks. No mass identification of these secondary tracks has been attempted.

The x_f and p_t distributions for K_S, Λ^0, $\overline{\Lambda}{}^0$, $K_S\Lambda^0$, and $K_S\overline{\Lambda}{}^0$ are consistent with those found from unbiased data[5] after corrections for acceptance are made. A check on the mass scale of this experiment is that the unconstrained K_S and Λ^0 masses agree with accepted values[6] within ± 1 MeV/c^2. As a further check we examine the $K_s\pi^\pm$ mass distributions and compare the observed $K^*(890)$ and $K^*(1420)$ masses and widths to those expected, given our mass resolution. The agreement is excellent.

In Fig. 1 is shown the $K_S\Lambda^0$ plus $K_S\overline{\Lambda}{}^0$ effective-mass distribution. This distribution and all subsequent mass distributions are fit with Breit-Wigner shapes for the resonances, and a background of the form

$$[a(M-M_t)+b(M-M_t)^2+c(M-M_t)^3]e^{-d(M-M_t)},$$

where M_t is the threshold mass. In performing the fits, the χ^2 contribution of each bin in a histogram is based on the difference between the number of events in that bin and the integral over the bin of the background plus resonance function. Masses and widths of known resonances[6] are fixed in the fits unless otherwise noted. When masses and widths are not well determined[6] the fixed values used in the fits are quoted in the text. The experimental resolution, as determined from observed widths of K_S^0 and Λ, is added in quadrature in all fits. In some cases it is necessary to exclude certain bins from the fits: either because

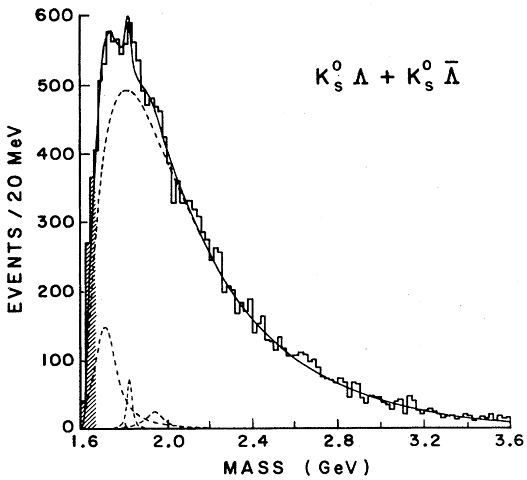

FIG. 1. Effective mass of the $K_S^0\Lambda^0$ or $K_S^0\bar{\Lambda}^0$ events. The dashed curves are fitted to background and resonances as described in the text; the solid curve is the sum of all the contributions. The shaded portion is excluded from the fit.

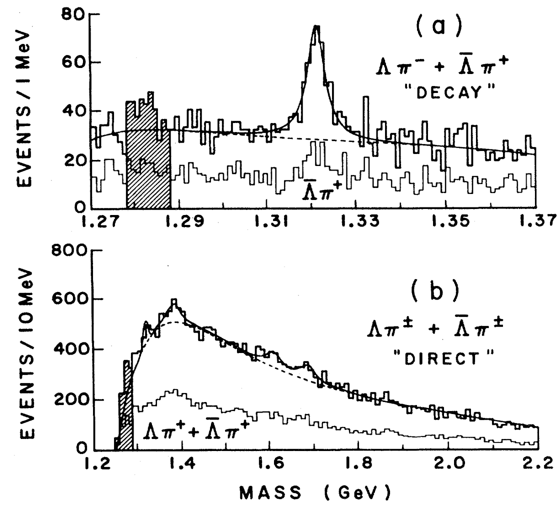

FIG. 2. (a). Effective mass of the $\Lambda^0\pi^-$ or $\bar{\Lambda}^0\pi^+$ entries for those pions which miss the primary interaction point by more than 3σ. The upper histogram is both charge combinations; the lower histogram is only the positive charge combination. The dashed curve is fitted to background as described in the text; the solid curve is the sum of all the contributions. The shaded portion is excluded from the fit. (b). Effective mass of the $\Lambda^0\pi^-$, $\Lambda^0\pi^+$, $\bar{\Lambda}^0\pi^-$, or $\bar{\Lambda}^0\pi^+$ entries for those pions which are within 3σ of the interaction point. The upper histogram is all charge combinations; the lower histogram is only the positive charge combinations. The dashed curve is fitted to background as described in the text; the solid curve is the sum of all the contributions. The shaded portion is excluded from the fit.

of the inadequacy of the polynomial-exponential model in the region of sharply rising phase space, or because of understood problems with the track-finding procedure. In all figures, excluded bins are indicated by shading.

The curve of Fig. 1 is such a fit with the resonances $N(1710)$, $\Gamma=120$ MeV/c^2, $\Xi(1823)$, $\Gamma=20$ MeV/c^2, and $\Xi(1940)$, $\Gamma=100$ MeV/c^2. The χ^2 per degree of freedom (DF) is 110/90. If the $\Xi(1940)$, the resonance for which the evidence is poorest (196$\pm$156 events), is not included in the fit, the χ^2 becomes 112 for 91 degrees of freedom. The evidence for the presence of the other two resonances is more compelling: 1422$\pm$356 events for the $N(1710)$, and 142$\pm$68 for the $\Xi(1823)$.

In Fig. 2 the effective mass of a Λ^0 or $\bar{\Lambda}^0$ and other single spectrometer tracks is shown. In Fig. 2(a) the track is a decay track, assumed to be a pion. Only the combinations $\Lambda^0\pi^-$ and $\bar{\Lambda}^0\pi^+$ are used. A clear $\Xi(1321)$ is seen, consisting of 350$\pm$35 entries for both charge combinations, with a width (4.3$\pm$0.7 MeV/c^2) consistent with the mass resolution. The χ^2/DF for this fit is 79/85. To check the accuracy of the mass scale, the fit was recalculated with the central mass allowed to vary. The result, 1321.4$\pm$0.3 MeV/c^2, is in excellent agreement with the world average[6] of 1321.3$\pm$0.13 MeV/c^2.

The Λ^0 or $\bar{\Lambda}^0$ plus "direct" track (assumed to be a pion) effective mass is shown in Fig. 2(b). In this case the $\Lambda^0\pi^\pm$ and $\bar{\Lambda}^0\pi^\pm$ charge combinations are used. A clear $\Sigma(1385)$ signal is observed (428$\pm$110 entries for all charge combinations) together with some $\Xi(1321)$ signal from decay tracks that were misidentified as direct tracks because of their forward decay topologies. The very low masses are excluded from the fit, as discussed above.

Weaker evidence for the presence of $\Sigma(1620)$ ($M=1613$, $\Gamma=35$ MeV/c^2) and $\Sigma(1690)$ ($M=1690$, $\Gamma=40$ MeV/c^2) is also present in the data. With these resonances included in the fit, the χ^2/DF is 62/45. Without them the best fit has χ^2DF=96/47. The best fit occurs for 384$\pm$86 $\Sigma(1620)$ events and 352$\pm$85 $\Sigma(1690)$ events when all charge combinations are included.

In Fig. 3 is shown the $\Xi^-\pi^+$ plus $\bar{\Xi}^+\pi^-$ mass distribution, where in this case and in what follows a Ξ^- is defined to be a $\Lambda^0\pi^-$ effective mass between 1318 MeV/c^2 and 1325 MeV/c^2. A clear $\Xi(1530)$ signal is seen with 43$\pm$8 entries. The χ^2/DF for the resonance plus background fit is 43/62 with the mass and width of the $\Xi(1530)$ fixed at the fitted values 1540 and 9.1 MeV/c^2, respectively.

The $K_S^0\Xi^-$ or $K_S^0\bar{\Xi}^+$ effective-mass distribution is shown in Fig. 4. A 2.5σ indication of $\Sigma(2250)$, 21$\pm$8 entries, is observed with fitted central mass 2236$\pm$6 and width 7^{+13}_{-7} MeV/c^2, both of which are consistent with the wide range of values previously reported.[6] The χ^2 for the overall fit is 69 for 67 degrees of freedom.

If the production dynamics of the resonances which are observed is such that baryons and antibaryons materialize out of the quark sea in the x_f region far from the region of target fragmentation, then one expects that the baryon-to-antibaryon ratio will be 1. Using our data alone this ratio can be studied with very little systematic bias for baryons of different strangeness. Since the x_f variation of our sensitivity, as noted previously, favors $x_f \geq 0.2$ and includes $0.0 \leq x_f \leq 0.2$, the data are in the pion fragmentation and central regions of production.

In order to study this question we have subdivided the data in Figs. 1 and 2 into different charge and baryon-number states and performed fits similar to those described above. For example, the lower histograms in

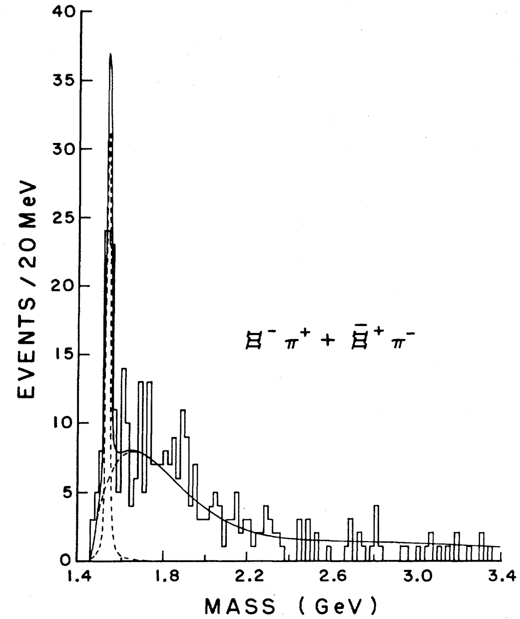

FIG. 3. Effective mass of the $\Xi^-\pi^+$ and $\bar{\Xi}^+\pi^-$ entries. The dashed curves are fitted to background and resonance as described in the text; the solid curve is the sum of all the contributions.

Fig. 2 show the combinations containing only positive charge. Only results for the most significant states are quoted.

For the $K_S^0\Lambda^0$ and $K_S^0\bar{\Lambda}^0$ data the resulting ratios are $\bar{N}(1710)/N(1710)=1.7\pm0.6$ and $\bar{\Xi}^0(1823)/\Xi^0(1823)=2.1\pm1.9$. The subdivided data of Fig. 2(a) yield the fitted ratio $\bar{\Xi}^+(1321)/\Xi^-(1321)=0.4\pm0.1$. Finally, the subdivided data of Fig. 2(b) yield the fitted ratio $\bar{\Sigma}^\pm(1385)/\Sigma^\pm(1385)=0.6\pm0.4$. Except for the $\Xi(1321)$, the ratios of antibaryon to baryon production are consistent, within statistics, with materialization out of the quark sea.

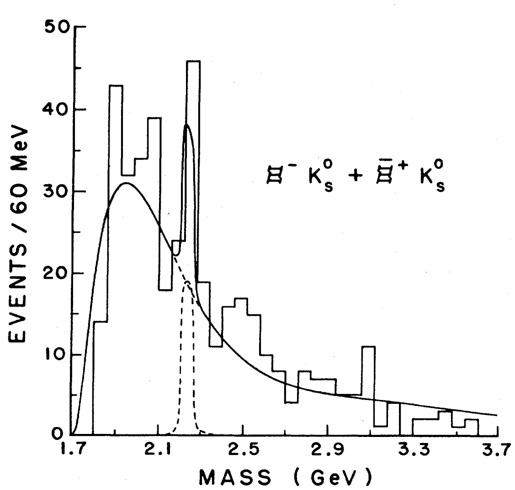

FIG. 4. Effective mass of the $\Xi^-K_S^0$ or $\bar{\Xi}^+K_S^0$ entries. The dashed curves are fitted to background and resonance as described in the text; the solid curve is the sum of all the contributions.

In order to probe the local compensation of strangeness, one may examine ratios of resonances with different strangeness but that are produced within the same final state. This procedure results in a reduced systematic bias. In this case the full data of Figs. 1 and 2 are used. In the $K_S^0\Lambda^0$ and $K_S^0\bar{\Lambda}^0$ final states the observed ratio, correcting for decay branching ratios, is

$$[N(1710)+\bar{N}(1710)]/[\Xi^0(1823)+\bar{\Xi}^0(1823)]=45\pm33 \ .$$

Using the $\Lambda^0\pi^\pm$ and $\bar{\Lambda}^0\pi^\pm$ data of Fig. 2(a), and correcting for Ξ appearing in Fig. 2(b) and for decay branching ratios, one finds the ratio

$$\frac{\Xi^-(1321)+\bar{\Xi}^+(1321)}{\Sigma^\pm(1385)+\bar{\Sigma}^\pm(1385)}=1.0\pm0.3 \ .$$

Variations of the geometric efficiency with mass, as determined by Monte Carlo methods, are considerably less than the statistical errors on these measured ratios.

One may compare these cross-section ratios to predictions from a phenomenological model.[7] This model, developed to codify nonleading particle production in hadron collisions, assumes factorization in rapidity and transverse momentum, and adds local compensation of quantum numbers in order to describe strange meson and antinucleon production within its framework. It has been applied successfully to strange-meson-resonance production at the CERN ISR.[8] The cross section for production of a mass m is given by

$$\sigma(m)=Ay_{\max}{}^2e^{-\alpha/y_{\max}{}^\beta}[M/(M+M_0)^\gamma] \qquad (1)$$

with $\alpha=5.13$, $\beta=0.38$, $\gamma=12.3$, and $M_0=2$ GeV/c^2. In this model, M is the mass of the simplest "composite" particle consistent with the production of m, and with local conservation of quantum numbers. The term $y_{\max}$ is the maximum rapidity that the composite particle can have when it recoils from another particle in the center of mass. In the calculations below we used a pion as the recoil, but the results are not sensitive to this choice.

Given local compensation of strangeness S, we have assumed values of M as follows: $M=1710$, $M=1385+m_K$, $M=1321+2m_K$, and $M=1823+2m_K$ for the $N(1710)$, $\Sigma(1385)$, $\Xi(1321)$, and $\Xi(1823)$, respectively. The predicted ratios are

$$[N(1710)+\bar{N}(1710)]/[\Xi^0(1823)+\bar{\Xi}^0(1823)]=34$$

and

$$[\Xi^-(1321)+\bar{\Xi}^+(1321)]/[\Sigma^\pm(1385)+\bar{\Sigma}^\pm(1385)]=0.24 \ .$$

The former ratio is in agreement with the data (45 ± 33), whereas the latter ratio is not in agreement with the data (1.0 ± 0.3).

For further discussion of our observations and comparison to other data, it is necessary to determine our cross-section normalization. We take the $K_S^0\bar{\Lambda}^0$ production cross section measured in a hydrogen-bubble-chamber exposure,[5] at 250 GeV/c π^-, and note that both the K_S^0 and $\bar{\Lambda}^0$ observed in that experiment appear to be produced centrally. Thus the production mechanism observed in the present experiment (see below) appears to be the same as the one providing the calibration point. We scale down

TABLE I. The parameters of the baryon states for this experiment which are plotted in Fig. 5.

State (MeV)	Decay mode	Composite mass (MeV)	Events	B (%)	(μb)
$N(1710)$	$K_S^0\Lambda^0$ or $K_S^0\bar{\Lambda}_0$	1710	1422±356	10±5	418±200
$\Sigma(1385)$	$\Lambda^0\pi^\pm$ or $\bar{\Lambda}^0\pi^\pm$	1879	428±110	88±2	23±8
$\Sigma(1620)$	$\Lambda^0\pi^\pm$ or $\bar{\Lambda}^0\pi^\pm$	2114	334± 86		
$\Sigma(1690)$	$\Lambda^0\pi^\pm$ or $\bar{\Lambda}^0\pi^\pm$	2184	352± 85		
$\Sigma(2250)$	$K_S^0\Xi^-$ or $K_S^0\bar{\Xi}^+$	2744	21± 8		
$\Xi(1320)$	$\Lambda^0\pi^-$ or $\bar{\Lambda}^0\pi^-$	2308	350± 35	100	41±4
$\Xi(1530)$	$\Xi^-\pi^+$ or $\bar{\Xi}^+\pi^-$	2518	43± 8	100	11±2
$\Xi(1820)$	$K_S^0\Lambda^0$ or $K_S^0\bar{\Lambda}^0$	2808	142± 68	45±10	9.4±4.4
$\Xi(1940)$	$K_S^0\Lambda^0$ or $K_S^0\bar{\Lambda}^0$	2928	196±156		

their measured cross section by the ratio of $(\ln s)^2$ to account for different beam momenta and determine that our sensitivity for uncorrected events is 68±31 events per microbarn.

Table I contains the observed states, the decay modes examined, composite masses, fitted numbers of events, branching ratios, and cross sections. The $N(1710)$ and $\Xi(1820)$ cross sections are directly normalized to unbiased data as noted above. The errors quoted on the cross sections reflect statistical errors and uncertainty in the $K_S^0\Lambda^0$ branching ratios. There is also an overall ~50% normalization uncertainty. For the $\Sigma(1385)$, $\Xi(1321)$, and $\Xi(1530)$ an additional set of assumptions is needed. The geometric efficiency correction for the pions is determined from the observed decay angular distributions. It is assumed that from the observed final state, e.g., $\Lambda^0K_S^0\pi^-$, one can extract the cross section for the state $\Lambda^0\pi^-$ by multiplying by 4: 2 for $[(K_S^0+K_L^0)/K_S^0]$ and 2 for $[(K^0+K^+)/K^0]$. No error has been assigned to this procedure. The quoted errors reflect only statistical errors and errors on branching ratios, added in quadrature.

Other data on inclusive baryon-resonance production in high-energy πN interactions are rather limited. In 147-GeV/c π^+p interactions, inclusive $\Sigma^{*+}(1385)$ was observed[9] with a cross section of 290±70 μb, and an upper limit was set on $\Sigma^{*-}(1385)$ production of 100 μb. At the ISR, $\Sigma^{*\pm}(1385)$ and $\Xi^-(1320)$ were observed[10] for $x_f \geq 0.4$ with cross sections 250, 40, and 9 μb for Σ^{*+}, Σ^{*-}, and Ξ^-, respectively. In 240-GeV/c pp interactions at $x_f=0.48$, $P_t=600$ MeV/c, the production of Ξ^-,$\bar{\Xi}^+$, Ω^-, and $\bar{\Omega}^+$ has been observed.[11] The latter two experiments have studied the proton fragmentation region, while the present experiment is sensitive to the entire forward hemisphere consisting of central and π^- fragmentation regions.

Figure 5 shows the relationship among our measured cross sections, the model,[7] and the other available data,[1,11,12] extrapolated to our center-of-mass energy using the model of Ref. 7. The curve is the cross-section prediction of the model as a function of the composite-particle mass M, where this mass is given in Table I. The factor A in Eq. (1) is taken to have the value 0.4×10^{-20} cm^{-2} which was used successfully in Ref. 11 to predict mesonic resonance cross sections in pp collisions at ISR energies. For the other data on ρ, $K^*(890)$, $K^*(1420)$, f', g, and Λ we have taken composite masses M of 770, $890+m_K$, $1420+m_K$, 1515, 1690, and $1115+m_K$, respectively. Although substantial discrepancies exist, the main trends of the data are consistent with this model, given our choice of M for meson and baryon states. This model incorporates central production of resonances and local conservation of strangeness and baryon number. The present data set extends the range of data in M and $\sigma(m)$ substantially.

Other information concerning production dynamics may be obtained from the x_f distributions. In Fig. 6 is shown the ratio of $\bar{\Lambda}^0$ and Λ^0 differential cross sections $d\sigma/dx_f$ as a function of x_f. The curve is a best fit[13] to analogous data on $\pi^-p\to\bar{p}X$ and $\pi^-p\to pX$ whose general behavior agrees with the present data. At $x_f\sim0$ the $\bar{\Lambda}^0/\Lambda^0$ ratio is ~0.5, perhaps indicating some contamination due to proton fragmentation. For $0.1\leq x_f\leq0.6$, $\bar{\Lambda}^0/\Lambda^0$ is ~0.75. In the region $x_f\geq0.6$ the $\bar{\Lambda}^0/\Lambda^0$ ratio increases, indicating that the $\bar{u}$ valence quark (shared with

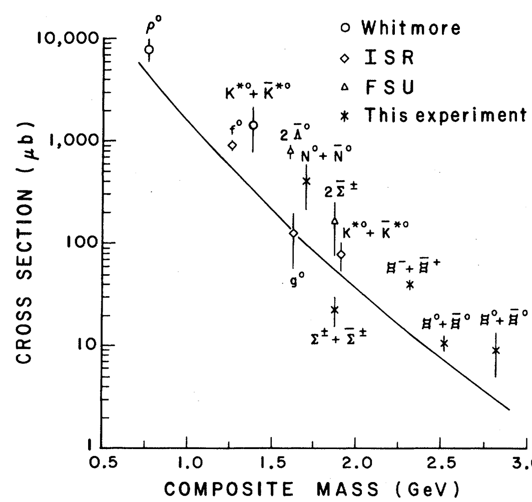

FIG. 5. Inclusive cross section for the production of mesons and baryons at 200-GeV/c laboratory momentum as a function of the composite mass, M, as defined in the text. The data is from the present experiment as well as Refs. 1 (Whitmore), 11 (ISR), and 12 [Florida State University (FSU)]. The error bars for this experiment do not include systematic uncertainties in our cross-section normalization. The curve is a calculation using the model in Ref. 7.

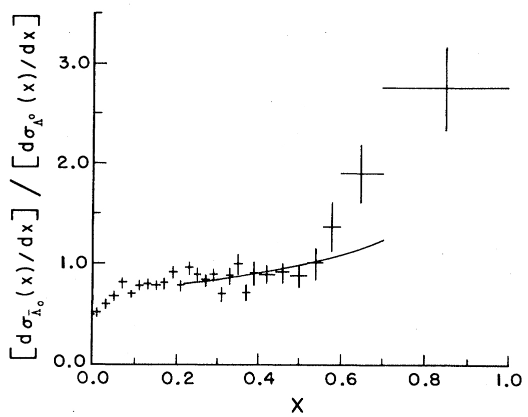

FIG. 6. The ratio of the $\bar{\Lambda}^0$ to Λ^0 differential cross section $d\sigma/dx$ plotted as a function of Feynman x. The curve is a fit to the $\bar{p}$-to-p ratio from Ref. 13.

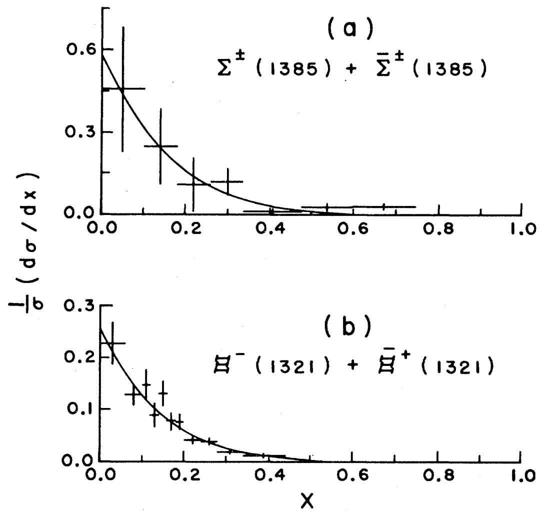

FIG. 7. The acceptance-corrected Feynman x distributions of $(1/\sigma)d\sigma/dx$ for (a) $\Sigma(1385)$ and (b) $\Xi(1321)$. The curves are best fits to the form $(1/\sigma)d\sigma/dx=\alpha(1-x)^n$.

the $\bar{\Lambda}^0$) in the π^- dominates over the d valence quark (shared with the Λ^0).

In Figs. 7(a) and 7(b) are shown the x_f distributions of the $\Sigma^{\pm}(1385)+\bar{\Sigma}^{\pm}(1385)$ and $\Xi^-(1321)+\bar{\Xi}^+(1321)$, after correction for experimental acceptance has been applied and background has been subtracted. The curves are fits to

$$(1/\sigma)d\sigma/dx=\alpha(1-x)^n ,$$

where n for the $\Sigma(1385)$ is 5.8 ± 1.7 and for the $\Xi(1321)$ is 6.7 ± 0.3. Although the available statistics do not allow any definitive statement about the relative shapes of these distributions, it can be seen that both states are produced in the central kinematic region, and that the exponents, n, are consistent with dimensional-counting schemes.[3]

In conclusion we have observed baryons with strangeness 0, 1, and 2 in π^-N interactions. Their production-cross-section ratios are consistent with central production and local quantum-number compensation. Their x_f distributions are consistent with analogous data from other channels, and also provide evidence of central production.

We thank the Fermilab staff, especially S. Hansen and R. Cantel, for their valuable help during this experiment. Z. Ma provided helpful support. The work was supported in part by Department of Energy contracts (Arizona, Florida State, Tufts) and National Science Foundation grants (Arizona, Notre Dame, Vanderbilt and Virginia Tech.).

---

*Operated by Universities Research Association Inc., under Contract with the United States Department of Energy.

†Permanent address: Dept. of Physics, Nanking U., Nanking, China.

‡Present address: Burr Brown Research Corp., 6730 S. Tucson Blvd., Tucson, Arizona 85706.

§Present address: High Energy Physics Lab., Stanford U., Stanford, California 94305.

**Former address: Florida State U., Tallahassee, Florida 32306.

††Present address: Motorola Inc., P.O. Box 2953, Phoenix, Arizona 85062.

[1]J. Whitmore, in *Proceedings of the 19th International Conference on High Energy Physics, Tokyo, 1978,* edited by S. Homma, M. Kawaguchi, and H. Miyazawa, (Phys. Soc. of Japan, Tokyo, 1979), p. 63.

[2]A. Krzywicki and D. Weingarten, Phys. Lett. **50B**, 265 (1974); R. Hagedron and J. Ranft, Nuovo Cimento Suppl. **6**, 169 (1968).

[3]R. Blankenbecler and S. J. Brodsky, Phys. Rev. D **10**, 2973 (1974); S. J. Brodsky and J. F. Gunion, *ibid.* **17**, 848 (1978).

[4]T. Y. Chen *et al.*, Phys. Rev. D **28**, 2304 (1983). For details of the experimental apparatus see C. Bromberg *et al.*, Nucl. Phys. **B134**, 189 (1978). For the configuration used in this experiment, see J. Poirer *et al.*, in *Multiparticle Dynamics 1981,* Proceedings of the XIIth International Symposium, Notre Dame, Indiana, edited by W. D. Shephard and V. P. Kenney (World Scientific, Singapore, 1982), p. 153.

[5]D. Bogert *et al.*, Phys. Rev. D **16**, 2098 (1977).

[6]M. Ross *et al.*, Phys. Lett. **111B**, 1 (1982).

[7]M. Bourguin and J. M. Gaillard, Nucl. Phys. **B114**, 334 (1976).

[8]A. Bohm *et al.*, Phys. Rev. Lett. **41**, 1761 (1978).

[9]D. Brick *et al.*, Phys. Rev. D **25**, 2248 (1982).

[10]S. Erhan *et al.*, Phys. Lett. **85B**, 447 (1979).

[11]M. Bourguin *et al.*, Z. Phys. C **5**, 275 (1980).

[12]S. Hagopian *et al.* (unpublished).

[13]D. Cutts *et al.*, Phys. Rev. Lett. **43**, 319 (1979).